DOI: 10.13009/EUCASS2023-745
Aerospace Europe Conference 2023 – 10TH EUCASS – 9TH CEAS

Flash-boiling effect on spray formed by two impinging jets

Łukasz Jan Kapusta *† *and Bartosz Kaźmierski* *
* *Warsaw University of Technology, Faculty of Power and Aeronautical Engineering*
Nowowiejska 21/25, 00-665 Warsaw, Poland,
lukasz.kapusta@pw.edu.pl – bartosz.kazmierski.dokt@pw.edu.pl
† Corresponding Author

Abstract
Although flash boiling has been highly interesting to many researchers, the vast majority of the studies have been limited to free sprays. In contrast, the effect of flash boiling on impinging jets is not yet understood.
In this study, we have aimed to fill these knowledge gaps and provide new insight into the global structures of sprays formed by two impinging liquid jets injected under flash-boiling conditions.
The results showed that even moderate flash boiling, in which unbroken liquid columns are still present, changes the global structure of the formed spray cloud. The colliding streams are shattered, and the spray is surrounded by the recondensing vapour.

1. Introduction

Impinging-jets nozzles' configuration has been proven to provide an efficient way to improve liquid jets' breakup and to mix the colliding liquids. Due to intensive collision, the mixing process is characterised by a high momentum and mass exchange so that even intact streams formed in Rayleigh or First wind-induced regime can break up into relatively small droplets and effectively create a spray cloud. Moreover, if the liquids are different, then during this collision process, they mix, and the two (or more) liquid substances are distributed over the whole spray cloud.

It has been observed that the streams with a smooth interface developed at low injection velocities, when impinged, tend to reflect from the impinging point, and the mixing process is limited. For higher flow velocities, which result in higher momentum and internal turbulence levels, the jets disintegrate into droplets just after the impingement point and do not entirely change the flow direction. In that case, more efficient mixing is observed, and the liquids emerging from different nozzles cross the impingement plane. This is called transmissive atomisation, which is most commonly observed in practical systems [1]. At higher velocities, when the jets' interfaces are disturbed, then the streams only partially interact, and more transmission is observed. This effect also depends on the jet diameter and impingement angle, with the bigger diameter and the wider impingement angle corresponding to a higher transmission. Imai [2] observed impinging water jet sprays to study mixing in a doublet (1-1) nozzles' configuration. They showed that the streams' interaction may differ depending on the pressure difference, which results in different exit velocities. However, despite the very different spray formation processes depending on the pressure drop along the nozzle, a common feature of those sprays was that the intact streams reach the collision point, which is the condition to achieve proper momentum and mass exchange.

For such conditions, a well-established understanding of the parameters governing the behaviour of liquid structures formed by the colliding streams exists. The collision dynamics and the structure of the formed spray primarily depend on the number of jets [3], the flow conditions and the physical properties of injected liquid [4], [5]. As in this study the focus is on doublet configuration, only the spray formation by the collision of two jets will be discussed. Such arrangements were studied the most [6], and the interaction of two liquid streams emerging from round nozzles of the same diameters is well understood [7]. In general, such arrangement leads to a generation of a planar liquid sheet which may behave in a different manner, e.g. forming quasi-stable chains or fishbones [8] or strongly time-dependent wavy structures [9]. It has been shown that the behaviour of the liquid sheet can be described by the dimensionless numbers, namely Reynolds and Weber numbers [8]–[10]. Li and Ashgriz [9] showed that for increased Reynolds number, the liquid sheet broke into droplets. Bush and Hasha [8] proposed a map presenting the dependence of liquid structures' types on the Weber and Reynolds numbers. At low values (of both Reynolds ad Weber numbers), the authors reported

DOI: 10.13009/EUCASS2023-745

structures in the form of oscillating streams and liquid chains. For the higher values, they observed spluttering of the chains and disintegration of the liquid sheet accompanied by intensive flapping.
Such a prediction of the collision dynamics and formed sheet's behaviour is possible when the streams travel along the nozzles' axes and collide at the axes' intersection point. However, there are several phenomena which can disrupt this process. When the liquid streams start to oscillate or break up into ligaments and droplets spread around the axes, the collision of the liquids travelling from different nozzles becomes less probable, and the momentum exchange process becomes less effective. It may happen when a liquid is injected into an environment of pressure lower than its vapour pressure. Then the flash-boiling phenomenon may occur, significantly changing the jet structure at the nozzle's exit. It is expected that the momentum and mass exchange will be worsened as instead of the collision of the intact streams travelling along nozzles' axes, an interaction of clouds of ligaments and droplets distributed over the larger volume will be observed.

The flash-boiling has been widely studied in terms of free jets and has been proven to alter the jet and spray properties strongly. It promotes smaller droplets' formation and improves evaporation. When a superheated liquid is injected into the environment of pressure below its vapour pressure, the vapour bubbles which are generated inside the liquid phase (streams, ligaments and droplets) expand rapidly and lead to "micro explosions", in which the liquid structures burst and form smaller versions [11], [12]. Recently, flash-boiling has been studied mainly in terms of high-pressure fuel injection in spark-ignition engines. In contrast, the low-pressure sprays weren't studied as extensively even though the first studies were performed several decades ago [11], [13]. Brown and York [11] observed a significant change in the jet's appearance when temperatures exceeded the saturation temperature. At the same time, they reported that the temperatures required to achieve that change needed to be higher by a considerable value than the boiling point at the corresponding ambient pressure. Similar observations were made by Peter et al. [13]. Kamoun et al. [14] reported an increasing spreading angle as a function of the saturation-to-ambient pressure ratio. Lamanna et al. [15] extended that study and proposed unified parameters to describe the behaviour of low-pressure flash-boiling sprays. Jin et al. [16] also reported the primary importance of the saturation-to-ambient pressure ratio, which also aligns with the previous findings for high-pressure sprays. They also reported that the injection pressures did have an influence on the global spray structure, with higher pressures resulting in a faster spray angle increase. Recent studies [17], [18] have shown that the influence of flash boiling on low-pressure sprays may be even more significant than in the case of high-pressure sprays. Those studies have shown that there was a substantial reduction of the droplet size and spray penetration while the spray angle was strongly increased. Additionally, the flash-boiling had a strong influence on the spatial distribution of droplets – the droplets of different sizes were more evenly distributed within a spray cloud. As far as the impinging-jets configuration is considered, the most important aspect which can alter the atomisation mechanism and the mixing process is a more distorted and shorter unbroken liquid column. As shown in [17], the length of the unbroken liquid stream can be strongly reduced already for a low degree of overheating; while the overall spray structure is not changed significantly. The streams of generated large droplets follow the initial injection direction while they are accompanied by the condensing vapour. This type of spray formation in [17] was called a hybrid injection combining the features of conventional and flash-boiling sprays.

Summing up, intensive momentum exchange between the two colliding liquids resulting in efficient atomisation and mixing is possible when the streams of injected liquids travel straight along the nozzles' axes and collide precisely at the intersection point. The existing knowledge on the behaviour of two colliding liquids concerns such conditions. However, when the liquid streams become wavy or shattered, the collision of the jets emerging from the different nozzles may become less probable, and the momentum exchange process is less effective. This may happen when a liquid is injected into an environment of pressure lower than its vapour pressure. In this case, rapid vaporisation (flash boiling) occurs, significantly changing the jet's structure at the nozzle's exit. In such conditions, the vapour bubbles generated inside the liquid stream expand rapidly and lead to the jet shattering and shortening of the unbroken liquid column.
Although flash boiling has been highly interesting to many researchers, and its influence on sprays is relatively well known, one may conclude that the vast majority of the studies have been limited to free sprays. In contrast, the effect of flash boiling on impinging jets is not yet understood.
In this study, we have aimed to fill these knowledge gaps and provide new insight into the global structures of sprays formed by two impinging liquid jets injected under flash-boiling conditions. As at a high superheat degree, the unbroken liquid column almost completely disappears, leading to a spray formation resembling the atomisation regime; in the case of impinging-jets configuration, it would lead to spray-spray interaction. In this study, we focus on intermediate levels of superheating in which still jet-jet interaction would be dominant. Therefore, in this work, the superheated liquid was injected in a so-called hybrid regime, in which the jets become shattered but still disintegrate into ligaments and large droplets following the initial injection direction while being accompanied by the recondensed flash-evaporated liquid.

DOI: 10.13009/EUCASS2023-745

2. Experimental setup

In this analysis, the spray structures were examined by studying the angles of the spray clouds. Experimental measurements were conducted using a high-speed camera (Photron SA1.1) and were categorised into three groups. The first group (cases 1.a - 5.a; see section *2.1 Experimental cases*) involved the injection of a single water jet. The second group (cases 1.b - 5.b) and the third group (cases 1.c - 5.c) included self-colliding jets, which were measured from two perpendicular directions (Fig. 1). The first direction was parallel to the plane of the jets, allowing for the measurement of the spreading angle of the sheet (α_1; see Fig. 1). The other direction was perpendicular to the plane of the jets, corresponding to the thickness angle of the liquid sheet (α_2; see Fig. 1).

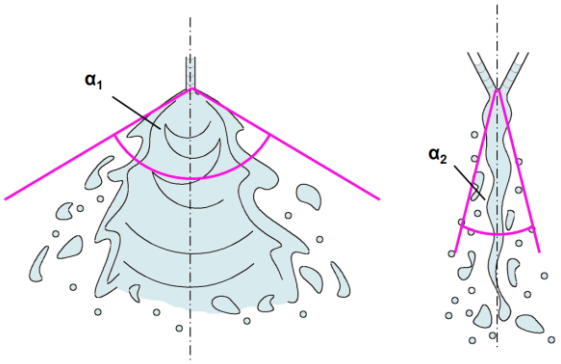

Fig. 1. Schematic representation of the angles of post-impingement structures formed after a collision of two liquid jets; **left:** spreading angle observed parallelly to the jets' plane (α_1); **right:** thickness angle observed perpendicularly to the jets' plane (α_2)

The injection head was equipped with two sets of nozzles arranged in pairs aligned with the main axes of the test stand (see Fig. 2.a). Each nozzle had a diameter of 0.7 mm. All jets collided at a single point in space, located 12 mm from the nozzle exit. The impingement angle was set at 30°. This nozzle configuration enabled the measurement of angles α_1 and α_2 without requiring any adjustments to the camera position (see Fig. 2). Consequently, all three measurement groups were captured using the same camera orientation, settings, and illumination.

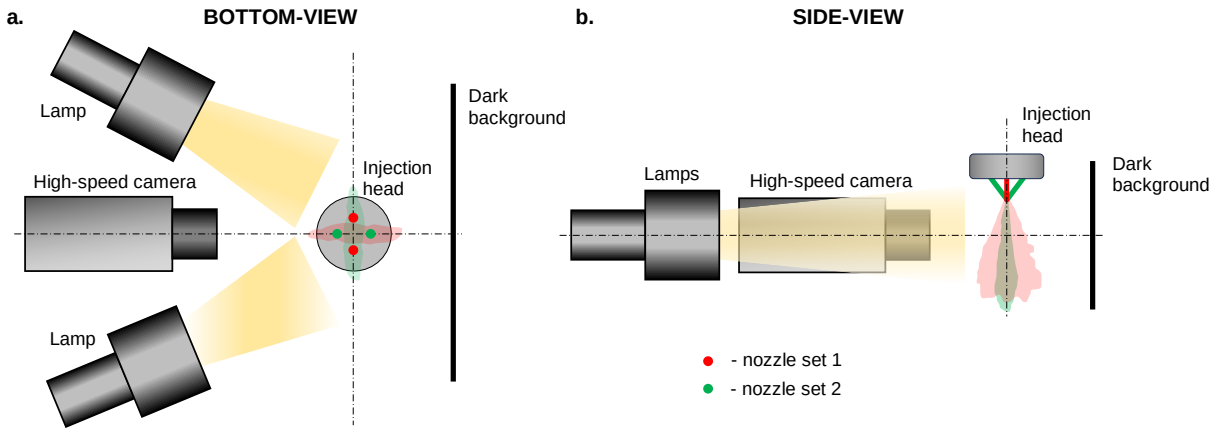

Fig. 2. The layout of the test stand; **a.** bottom view, **b.** side view; red colour – spray cloud from the nozzle set 1; green colour – spray cloud from the nozzle set 2; dimensions not-to-scale

An important aspect of this analysis was the precise temperature control of the injected liquid (water). The water was preheated in a cylindrical pressure vessel that contained four independent electric heaters. The vessel was thermally insulated with a 20-mm thick silica cover and lined with aluminium foil. The vessel was connected with the injection head by steel tubes of the same length with a 4-mm internal diameter. The outer walls of these channels were heated using silica tapes and thermally insulated with fibreglass silicone-covered sleeves. The temperature control of the injection head was achieved by a cooling jacket with circulating silicone oil and a coolant circulator (Huber Kiss K6). Temperature measurements of the water were taken using K-type ungrounded thermocouples. Two thermocouples were placed in the water vessel, with one positioned roughly in the centre of the vessel's volume and the other at the outlet from the vessel. The tip of the last thermocouple was placed inside one of the channels of the nozzle set 1, approximately 10 mm from the nozzle's exit (Fig. 3). Each nozzle was independently operated using a solenoid valve (Bürkert 0255-23279). The experimental setup included two LED lamps (Aputure® Amaran 200D) positioned

DOI: 10.13009/EUCASS2023-745

symmetrically on both sides of the camera. These lamps, along with additional Fresnel lenses (Aputure® Fresnel 2X), were directed towards the sprays (Fig. 2).

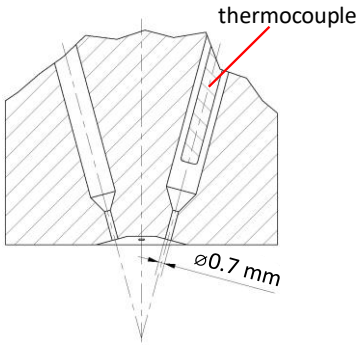

Fig. 3. Simplified section view of the injection head (nozzle set 1) depicting the location and size of the internal thermocouple

2.1 Experimental cases

The experiments were conducted under ambient-air conditions at an injection pressure of 5 bar. The flash-boiling effect was achieved by increasing the temperature of the water prior to the injection. Five different cases were selected for the analysis, as outlined in Table 1. Precise temperature values are reported in the results section (Table 2.), as the temperature was calculated after the experiment based on the indication of the thermocouple in the injection head. In case 1, the water temperature remained well below the boiling point in ambient conditions, resulting in a typical subcooled injection. Case 2 aimed to reach a water temperature slightly below the boiling point, and case 3 close to the boiling point in ambient conditions. In cases 4-5, the water temperature was set to exceed the boiling point in ambient-air conditions.

Table 1. Experimental cases defined before taking the measurements

Case	Temperature conditions	Comment
1.a/b/c	<< boiling point	
2.a/b/c	< boiling point	**.a** - single nozzle
3.a/b/c	~ boiling point	**.b** - two, self-colliding jets; spreading angle (α_1)
4.a/b/c	> boiling point	**.c** - two, self-colliding jets; thickness angle (α_2)
5.a/b/c	>> boiling point	

The temperature of the oil circulator was intentionally set higher than the desired water temperature by 6-10 °C to compensate for the heat losses in the injection head. Similarly, the temperature of the heating tapes covering the tubular connections was raised by 40 °C in case 1 and by 45 °C in the remaining cases.
The injections were performed once the temperature readings at the outlet and centre of the vessel had stabilised over time, and the temperature difference between the two measurement locations in the vessel was below 4 °C (Fig. 4). Ultimately, the cases for the analysis were selected after the measurements to meet the requirements defined in Table 1.

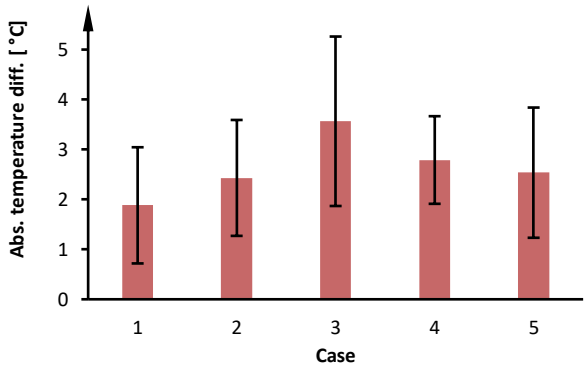

Fig. 4. Absolute temperature differences inside the water vessel in cases 1– 5; the presented values were derived by time-averaging over 100 ms before the injection and series-averaging; error bars represent standard deviations of time-averaged values

DOI: 10.13009/EUCASS2023-745

2.2 Measuring procedure

The measurements included three series of images for each case, with a duration of 0.7 seconds. The camera had a frame rate of 10,000 frames per second. The measurement of water temperature was synchronised with the opening of the solenoid valves and image acquisition.
During the measurements, it was observed that the temperature indicated by the thermocouple inside the injection head decreased after the solenoid valves were opened, despite the 0.8-second pre-injections. This suggested that the tubular channels were affected by cooling effects, and the time elapsed between the pre-injection and the actual recording was too long (on the order of seconds) to compensate for this cooling.
Therefore, additional temperature measurements were taken inside the injection head and vessel during a longer injection event lasting 20 seconds, using a single nozzle and conditions from case 1.a. to investigate these temperature deviations (see Fig. 5.).

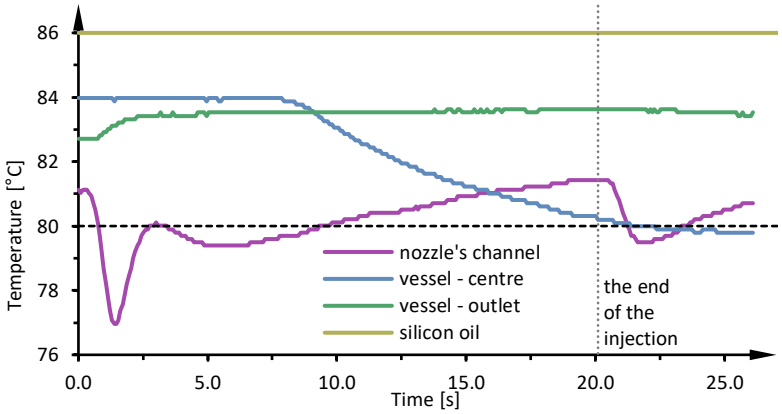

Fig. 5. Temperatures of water (measured inside the injection head and vessel) and heating oil in the circulator for the 80 °C case; injection duration 20 s, start of injection at 0.1 s

Inside the nozzle channel, a sudden temperature drop occurred immediately after opening the solenoid valves, indicating a potential decrease in temperature inside the tubular channels. After 1.4 seconds, the temperature started to rise as the tubular channels were fully filled with fresh, preheated water from the vessel. The temperature rise stopped at around 2.5 seconds, reaching a similar level to the stable value observed at the end of the measurement. The results showed a constant temperature of 84 °C at the centre of the vessel. However, approximately 8 seconds after the start of the injection, the temperature decreased due to the water level falling below the thermocouple's tip and the subsequent gas expansion inside the vessel. The temperature at the vessel's outlet was initially lower (approximately 82.7 °C) than at its centre, resulting from convection and buoyancy forces. Around 0.6 seconds after the start of the injection, the temperature at the vessel's outlet started to increase and remained at 83.5 °C until the end of the recording. Based on these measurements, the measuring procedure was modified, and the image acquisition in cases 4 and 5 was finally delayed by 2.5 seconds after the opening of the solenoid valves.

2.3 Image postprocessing

The angle of the spray structures were determined based on the filtered and binarised images. To reduce potential noises, the image post-processing was started with background subtraction. The background image was the first image in each series, where no injection was registered yet (Fig. 6 b.), and it was subtracted from all images in a given series. However, light reflection and scattering from the water structures during the injections introduced additional noise in the images even after background subtraction (Fig. 6 c.). To address this issue, all pixels above the spray origin (the nozzle location for single-jet cases and the collision point for impinging-jet cases) were removed (Fig. 6 d.). The images were then binarised (Fig. 6 e.) using the method proposed by Otsu et al. [19], with the binarisation threshold evaluated individually for each picture to maximise interclass variance.
For the binarised images, two sides of the considered angle were iteratively determined with an accuracy of 0.1° each until the total fraction of 10% of white pixels where cut-off from both sides of the expected spray structure (Fig. 6 f.). The sides originated from the nozzle's exit in the case of single jet (with additional 2-pixel offsets outwards), and from the collision point in the cases of self-impinging jets (with the analogous 2-pixel offsets outwards this point). Additionally, intensity plots were generated, where the colours represented the intensity of grayscale images (Fig. 6 h). These intensity plots highlighted areas with a high concentration of bright pixels.

DOI: 10.13009/EUCASS2023-745

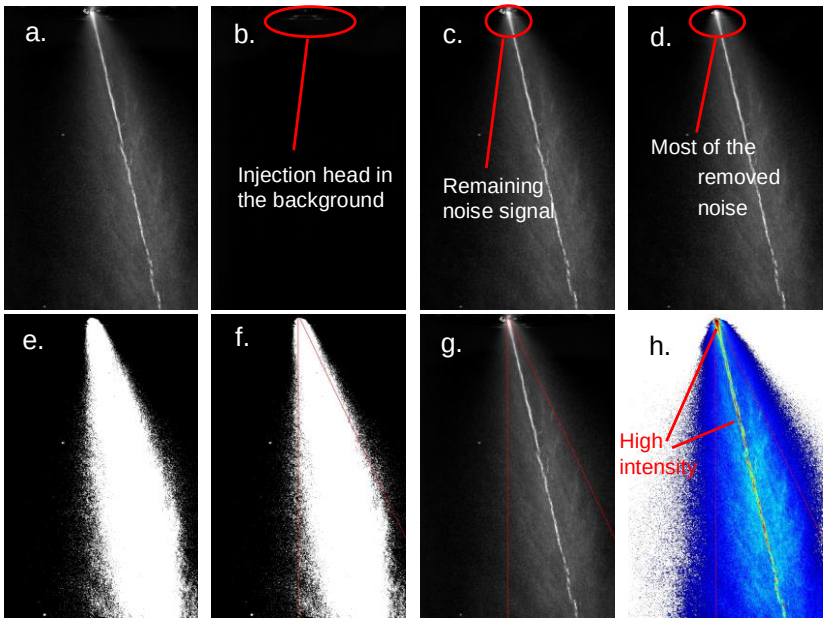

Fig. 6. Example of image post-processing steps (case 5.a, image obtained at 0.4 s at the start of recording): **a.** raw image; **b.** background image; **c.** image after the background subtraction; **d.** filtered image; **e.** binarised image; **f.** binarised image with plotted angle; **g.** raw image with plotted angle; **h.** intensity plot

3. Results

The liquid structures formed through the collision of two symmetrical water jets under a similar injection pressure of approximately 5 bar were evaluated by examining the spray angle. Different water temperatures were tested to investigate both conventional and flash-boiling injections. Furthermore, the behaviour of a single water jet from one of the nozzles was examined under analogous conditions to self-impinging jets.

3.1 Actual injection conditions

Water temperature control involved various heating elements such as the vessel's heaters, heating tapes, and oil circulation. To determine the actual temperature of the liquid during the injection, the indications of the thermocouple inside the injection head were time-averaged over a 0.4-s period, and this period corresponded with the image registration. These averaged values were then further averaged for three repetitions, and the final results are presented in Table 2.

Table 2. The calculated liquid temperature based on the indications of the thermocouple from the nozzle set 1

Case	Average temperature [°C]
1.c	80.6
2.c	98.7
3.c	100.3
4.c	102.1
5.c	111.2

Reaching desired temperatures required several repetitions of the tests with different settings as the calculated temperatures deviated from the set values, with more significant deviations observed at higher-temperature cases. In case 1, the average water temperature was around 81 °C, which aligned closely with expectations. In case 2, the average temperature also matched the set value. Significant deviations from the target temperatures were observed in cases 3.c - 5.c, with the series- and time-averaged temperatures being much lower than the set values. The decreased temperature readings can be attributed to two fact that different temperature drops may occur under different conditions, indicating that the dynamics of temperature changes presented in Fig. 5 is only applicable to the lowest-temperature case. In other words, higher temperatures of water preheating may be necessary to compensate for increased heat losses.

DOI: 10.13009/EUCASS2023-745

3.2 Self-impinging jets

Figure 7 shows the structures of the impinging-jets sprays visualised in two different directions.

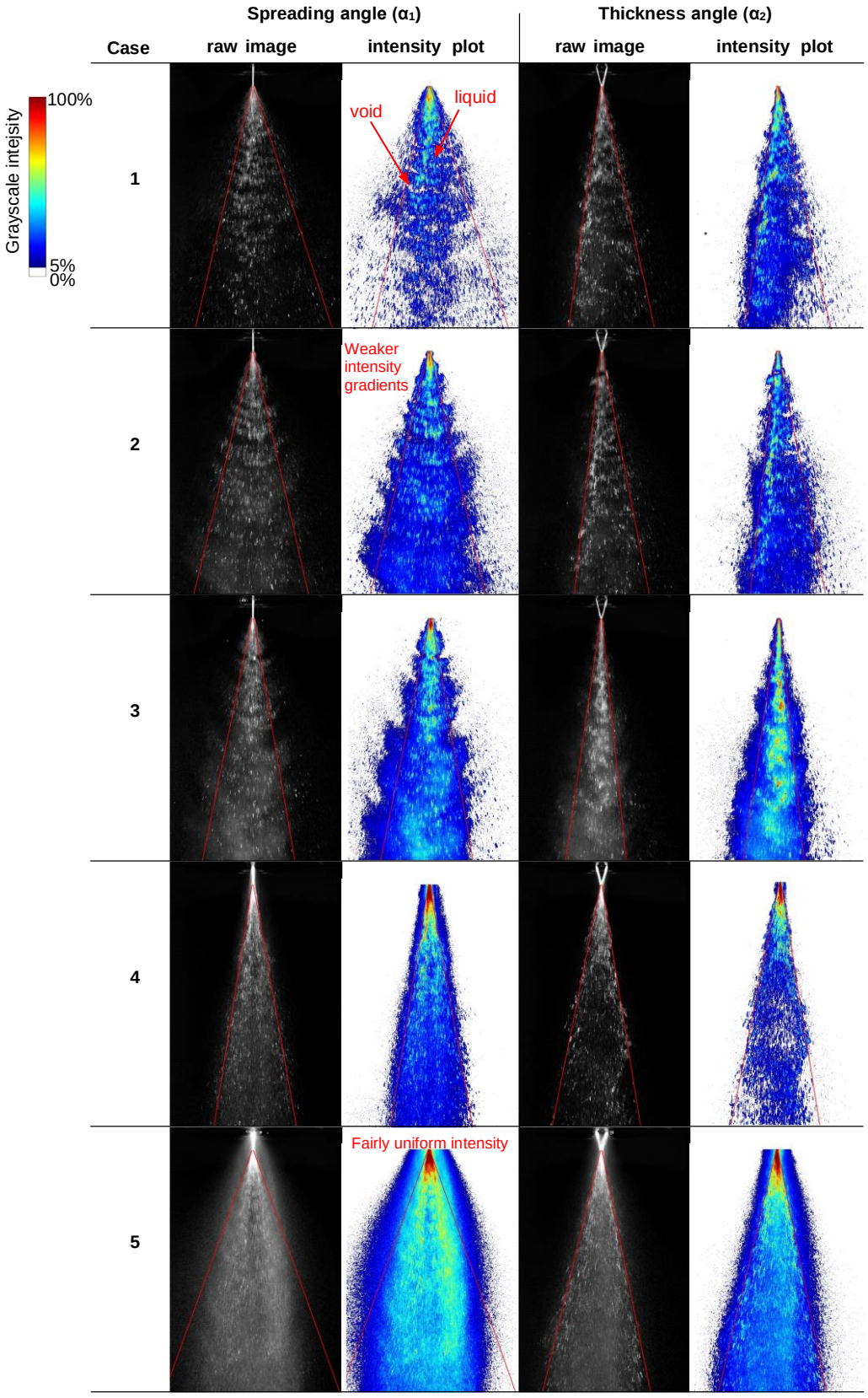

Fig. 7. Raw instantaneous images and corresponding intensity plots of impinging-jet cases with the resultant angle lines

DOI: 10.13009/EUCASS2023-745

The images show significant changes in the spray appearance depending on the temperature, manifested mainly by the gradually disappearing signal gradients between the liquid structures and the void spaces along the spray cloud with the increasing temperature. It shall be related to the change in the mechanical breakup and the presence of condensing vapour within the whole spray cloud, especially at the highest temperature (case 5).

Such behaviour did influence the angles of the formed spray cloud. The spreading angle α_1 (see Fig. 8.a) showed a slight decrease (-4%) as the water temperature increased from 80.6 °C to 98.7 °C. Further elevating the water temperature to near-boiling conditions (100.3 °C; case 3.b) resulted in a sudden narrowing of the spray. The narrowing of the spray further propagated after the slight temperature increase to approximately 102.1°C. When the moderate flash-boiling conditions were reached (111.2 °C; case 5.b), the spreading angle α_1 increased significantly (+22.5% compared to the subcooled case 1.b).
A similar trend was observed for the thickness angle α_2 (see Fig. 8.b). It decreased from 17.7° to 15.2° (-14.2%) as the water temperature changed from 80.6°C to 98.7°C. However, unlike the spreading angle α_1, the thickness angle α_2 began to increase with temperature in cases approaching boiling conditions. The angle α_2 continued to increase, demonstrating an almost linear rise between cases 2.c-5.c, eventually reaching a value of 27.4° under flash-boiling conditions (+55% compared to the subcooled case 1.c).
These effects are supposed to be associated with a more shattered stream and less intense momentum exchange.

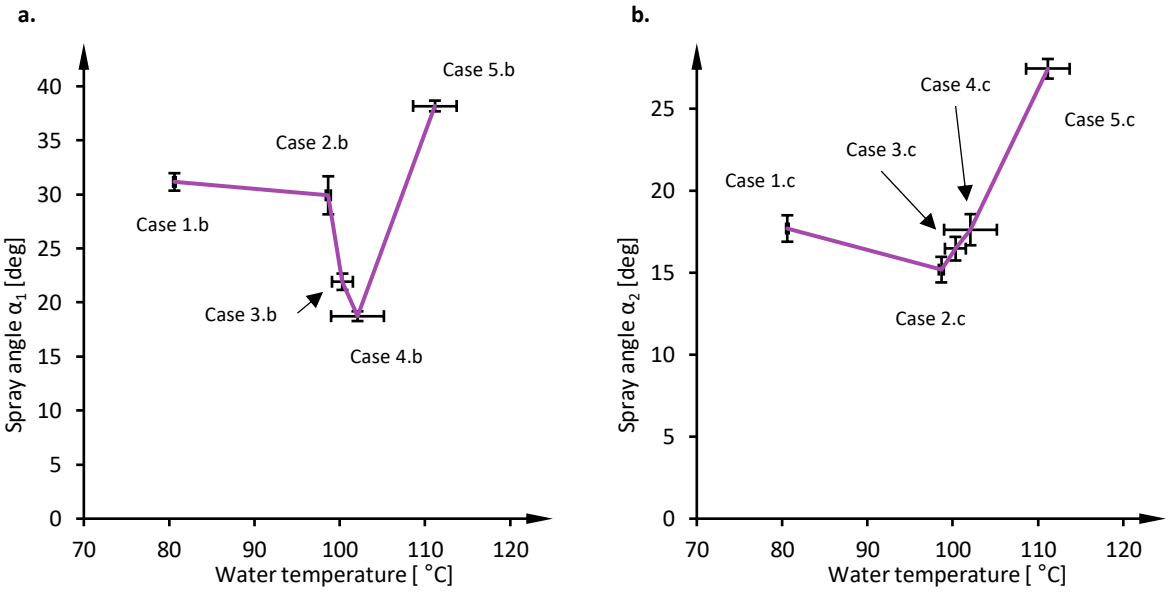

Fig. 8. Spray angles after series- and time-averaging; horizontal error bars represent standard deviations of time-averaged water temperatures inside the nozzle channel in reference cases 1.c – 5.c; vertical error bars are standard deviations of series-averaged spray angles; **a:** spreading angle α_1; **b:** thickness angle α_2

In the case of conventional, subcooled injection (80.6°C; case 1), self-impinging water jets produced fragmented liquid sheets intensely disintegrating into droplets and ligaments (see Fig. 7; case 1). This observation is in accordance with other studies [8], [20], which indicate intense atomisation in the case of high Reynolds and Weber numbers of liquid jets. The water streams did not disintegrate before collisions, interacting precisely at a single point in space. The increase of the water temperature to near-boiling point (100.3 °C; case 3) resulted in the generation of condensed steam. However, the jets prior to the collision seemed to remain unaffected. Moreover, the shape of the spray clouds and the wave structures also remained similar, with only slightly lower gradients between the low- and high-intensity areas. Increasing the water temperature slightly above the boiling point resulted in a notable widening of the liquid jets upstream from the collision point (102.1°C; case 4). The spray structure also contracted, and the distinctive wave pattern diminished. The spray resembled the conical structure typically formed by specific single-nozzle injectors. Exceeding the boiling temperature in case 5 (water temperature of 111.2°C) triggered the flash-boiling effect, leading to wider water streams prior to the collision and to the significant broadening of the resulting spray structures compared to the lower-temperature cases.
The simultaneous broadening of both angles (especially the thickness angle α_2) and the widening of the liquid jets prior to the collision may suggest that the effect of strong broadening of the spray angles (measured from the collision point) in flash-boiling conditions is related to a strong presence of condensed vapour which surrounds the jets. To verify this assumption the final part of the work focused on the analysis of the single-stream behaviour in similar conditions. This issue is discussed in the next section.

DOI: 10.13009/EUCASS2023-745

3.3 Single-jet injection

Figure 9 displays selected frames of single-jet injections with marked spray angles. The images clearly show that also, for a single jet, there is a substantial spray widening at the highest temperature conditions (case 5.a). In subcooled conditions (81.6 °C; case 1.a), the stream remained mostly uninterrupted with only minor disturbances. When the water temperature approached the boiling temperature (100.3 °C; case 3.a), the condensed vapour became visible, characterised by low-intensity pixels (blue colour on the intensity plots in Fig. 9).

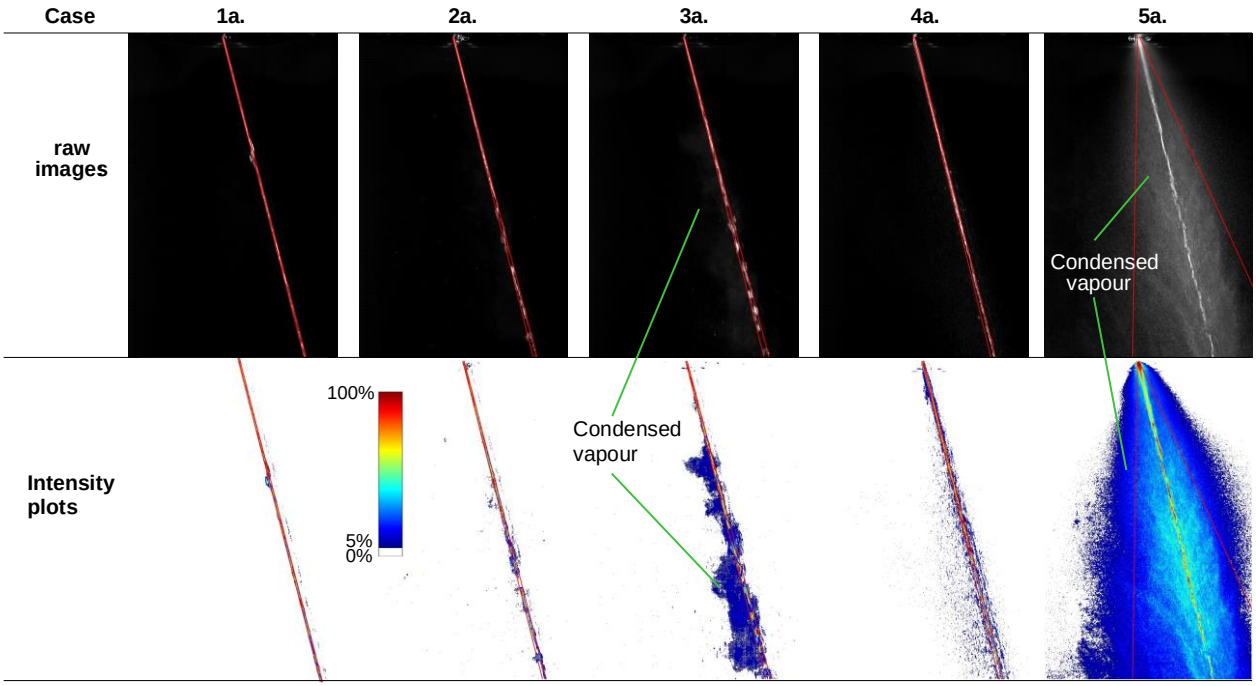

Fig. 9. Comparison of instantaneous raw images (top row) and intensity plots of single-jet cases (bottom row) with marked angles (red lines)

The angles were determined for each frame (as displayed in Fig 9); however, they were averaged over time and repetitions to compare the cases.

The time evolution of the determined angles of the single jets is shown in Fig. 10. These evolutions were derived from the averaging of three measurement series per each case. In cases 1.a-3.a, the initial high values observed are attributed to the water starting to appear in the images. Due to the presence of isolated individual pixels, the estimated angle values were distorted and appeared higher at the initial stage. However, these values stabilised after approximately 0.2 seconds once the jets were fully formed and the initial ligaments and blobs were no longer present in the images. In cases 4.a-5.a, the angle values remained stable from the beginning of the recorded evolution, resulting from the applied delay between the opening of the solenoid valve and the start of the image recording.

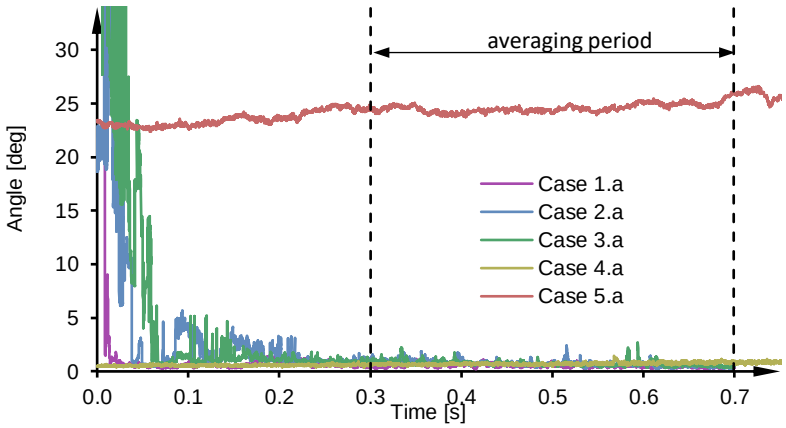

Fig. 10. The evolution of the angle of a single jet; time is referenced to the start of the injection in cases 1.a-3.a, and the start of image capturing in cases 4.a-5.a

DOI: 10.13009/EUCASS2023-745

In the subsequent step, the angles averaged over the series were further averaged within the time range of 0.3 to 0.7 seconds (see Fig. 10), and the results are presented in Fig. 11.

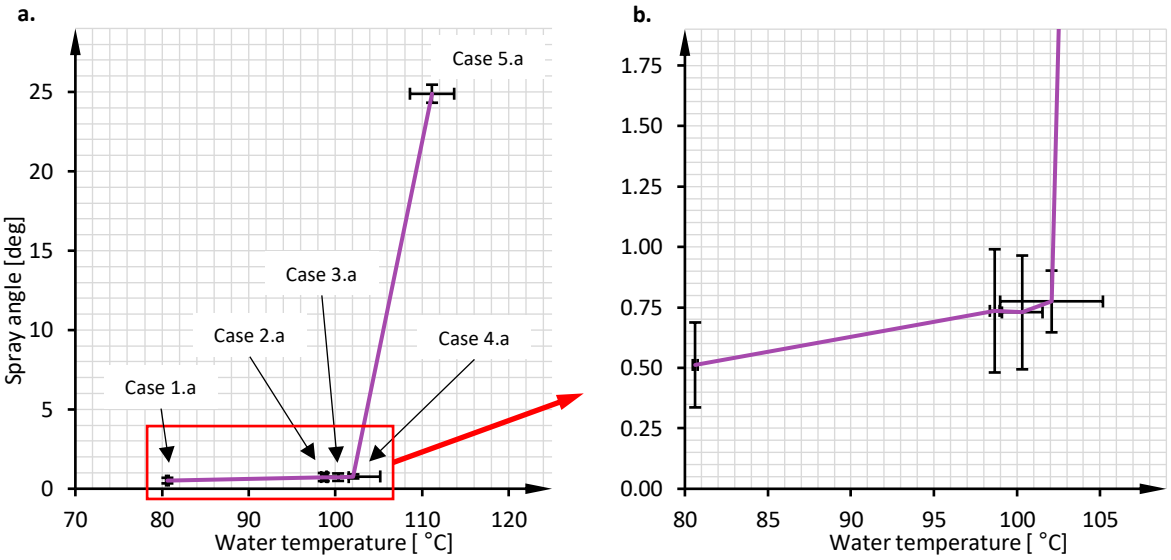

Fig. 11. Spray angles after series- and time-averaging; horizontal error bars represent standard deviations of time-averaged water temperatures inside the nozzle channel in reference cases 1.c – 5.c; vertical error bars are standard deviations of series-averaged spray angles; **a:** all considered cases 1.a – 5.a; **b:** zoom into cases 1.a – 4.a

For the subcooled and near-boiling cases, the obtained angles ranged from 0.5° (81.6 °C; case 1.a) to 0.8° (102.1 °C; case 4.a), which means that no significant jet breakup nor vapour generation (and recondensation) was observed in those cases. A significant increase in the angle was observed when the liquid temperature exceeded the boiling temperature by approximately 11 °C (case 5.a). In such conditions, a substantial amount of condensed vapour around the liquid core was observed (see Fig. 9). These findings are consistent with previous studies conducted on low-pressure, pulsed injections under flash-boiling conditions [17]. Exceeding the boiling temperature broadens a liquid structure, particularly near the injector [18]. However, it was reported [17], [21], [22] that a temperature increase of at least 15-25°C above the boiling temperature is necessary to observe the full effects of a flash-boiling injection. When the liquid temperature is raised only slightly below the boiling temperature, the spray structure enters a transitional stage, which in the following analysis was identified by the presence of a distinct liquid core.

3.4 Comparison of self-impingement and flash-boiling effects

The visualisation of spray structures formed by impinging jets and single jets (free sprays) allowed us to speculate on the implications of self-impingement and flash boiling. It was observed that the angle widening effect in the superheated regime (case 5) was similar for single-jet and imping-jets cases, even though the angle measured in a single jet between subcooled (case 1.a) and flash-boiling (case 5.a) conditions exhibited a much greater increase compared to impinging jets. However, this resulted from a greater angle value in the subcooled case. This similar effect could suggest that flash-boiling affects the spray angle mainly due to the strong generation of vapour, which partially recondensed, creating a cloud surrounding the stream of the injected liquid intensively scattering light (see Fig 9, case 5). However, the qualitative analysis of the images showed that superheating also affected the collision mechanism. As shown in Fig. 7, the intensity gradients along the spray related to the wavy structures gradually disappeared with increasing temperature. This suggests that the effect of flash-boiling is twofold.
It needs to be noted that for the impinging jets, the sprays were not symmetrical, and the sides of the determined angles were inclined to the axis of the injection head differently – in the subcooled case as well, which could suggest either dissymmetry in the collision or in the illumination. However, the single jet injection shows only a minor dissymmetry (see Fig 12, case 5.a), which might indicate a dissymmetry in the collision.
The significant increase in the thickness angle α_2 for case 5.c is believed to result from the breakup and dispersion of the jets before the collision, leading to weaker momentum exchange during the collision, indicating the influence of the flash-boiling effect (see Fig. 7, raw images). However, the comparison of the single and impinging-jet flash-boiling cases (Fig 12.) reveals that the presence of vapour was lower in case 5.c compared to a single jet, and distinct droplet traces remained visible downstream of the impingement point. Therefore, the observed effects cannot be assigned to a strong presence of the condensed vapour, which is visible in the single-jet case.

DOI: 10.13009/EUCASS2023-745

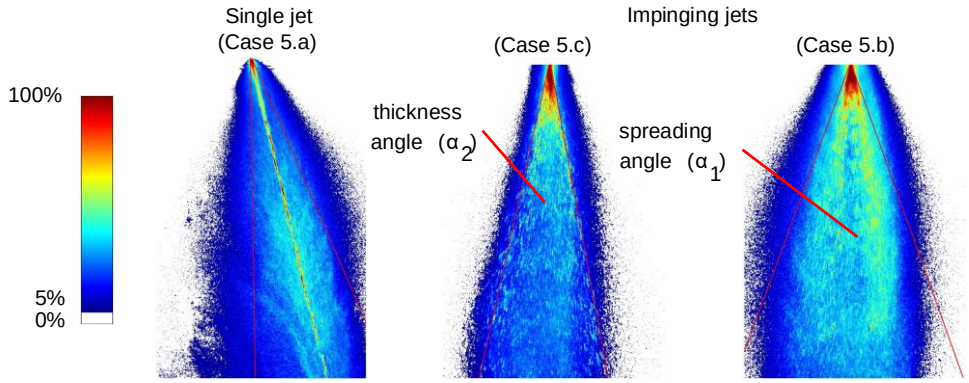

Fig. 12. The comparison of intensity plots for the flash-boiling cases; the binarisation threshold of 0.2 was applied

The observation of the spreading angle α_1 (case 5.b) showed greater vapour development than the thickness angle (case 5.c). However, the spray shape resembled other impinging-jet cases with distinct droplet traces. Based on these findings, it was assumed that the change in the impingement process induced by the flash boiling dominated the spray behaviour, and the overall effect on the spray cloud could not be solely associated with condensed vapour.

4. Conclusions

In this study, we investigated the effect of flash-boiling on the spray structures formed by self-impinging water jets in ambient conditions. The flash-boiling effect was controlled by adjusting the temperature of the water prior to the injection. The maximum registered temperature of 111.2 °C resulted in moderate flashing. Additionally, the angles of a single water jet formed under analogous conditions were measured as well. Based on the results, the following observations and conclusions were made:

- The highest temperature case (~111.2 °C) led to a significant increase in all investigated angles, namely the spreading and thickness angles of the post-impingement spray clouds.
- As expected based on previous experiments on pulsed injection [17], in the case of a single jet, a liquid core was present for the highest water temperature (~111.2 °C), which corresponds to a moderate flash-boiling.
- However, the measured angle was strongly widened as well by the presence of condensed vapour.
- Nevertheless, the condensed vapour couldn't explain this effect alone, as in the impinging-jet cases, the intensity gradients along the spray related to the wavy structures gradually disappeared with the temperature.
- Both angles of the spray structures from self-impinging jets decreased as the water temperature increased to approximately 98.7 °C, with the substantial drop in spreading angle α_1, which could suggest decreased momentum exchange between the colliding jets – possibly by probably more distorted structures of the jets prior to the impingement, which shall be verified with microscopic imaging of the jets.
- Based on the droplet traces which could be observed in the whole spray cloud in the case of impinging jets (contrary to the single-jet case) under the highest considered temperature, it can be assumed that the overall effect of moderate flash-boiling on the spray cloud, primarily depended on the flash boiling-induced change in the collision process. At the same time, the presence of condensed vapour could not explain this effect alone.

The results showed that even moderate flash boiling, in which unbroken liquid columns are still present, changes the global structure of the formed spray cloud. The colliding streams are shattered, and the spray is surrounded by the recondensing vapour. At the same time, the results indicated the need for further research to visualise the microscopic structure of the jets' interphase prior to the collision and explain the phenomena behind the differences observed in the various temperature regimes. Moreover, the pressure trace and the mass flow rate should also be verified during the injection to conclude on the Weber and Reynolds number effects, as these parameters were shown to play the primary role in the mechanical breakup of impinging jets. This is planned to be carried out in the near future.

Acknowledgements

This research was funded in whole or in part by the National Science Centre, Poland, within the framework of the SONATA programme, grant number: 2020/39/D/ST8/00947. For the purpose of Open Access, the author has applied a CC-BY public copyright licence to any Author Accepted Manuscript (AAM) version arising from this submission.

DOI: 10.13009/EUCASS2023-745

References

[1] N. Ashgriz, "Impinging Jet Atomization," in *Handbook of Atomization and Sprays: Theory and Applications*, N. Ashgriz, Ed. Boston, MA: Springer US, 2011, pp. 685–707. doi: 10.1007/978-1-4419-7264-4_30.

[2] K. Imai, "The Distributions of Flow Rate and Mixing Ratio of Two Impinging Jets," *Bull. JSME*, vol. 8, no. 31, pp. 441–452, 1965, doi: https://doi.org/10.1299/jsme1958.8.441.

[3] B. Pizziol, M. Costa, M. Panão, and A. Silva, "Multiple Impinging Jet Air-Assisted Atomization," 2017. doi: 10.4995/ILASS2017.2017.4737.

[4] M. Heidmann, R. J. Priem, and J. C. Humphrey, "A study of sprays formed by two impinging jets," 1957.

[5] M. M. Avulapati and R. Rayavarapu Venkata, "Experimental studies on air-assisted impinging jet atomization," *Int. J. Multiph. Flow*, vol. 57, pp. 88–101, 2013, doi: https://doi.org/10.1016/j.ijmultiphaseflow.2013.07.007.

[6] X. Chen and V. Yang, "Recent advances in physical understanding and quantitative prediction of impinging-jet dynamics and atomization," *Chinese J. Aeronaut.*, vol. 32, no. 1, pp. 45–57, 2018, doi: 10.1016/j.cja.2018.10.010.

[7] D.-J. Ma, X.-D. Chen, P. Khare, and V. Yang, "Atomization patterns and breakup characteristics of liquid sheets formed by two impinging jets," in *49th AIAA Aerospace Sciences Meeting including the New Horizons Forum and Aerospace Exposition*, doi: 10.2514/6.2011-97.

[8] J. W. M. Bush and A. E. Hasha, "On the collision of laminar jets: fluid chains and fishbones," *J. Fluid Mech.*, vol. 511, pp. 285–310, 2004, doi: DOI: 10.1017/S002211200400967X.

[9] R. Li and N. Ashgriz, "Characteristics of liquid sheets formed by two impinging jets," *Phys. Fluids*, vol. 18, no. 8, p. 87104, 2006, doi: 10.1063/1.2338064.

[10] N. Yasuda, K. Yamamura, and Y. H. Mori, "Impingement of liquid jets at atmospheric and elevated pressures: an observational study using paired water jets or water and methylcyclohexane jets," *Proc. Math. Phys. Eng. Sci.*, vol. 466, no. 2124, pp. 3501–3526, 2010.

[11] R. Brown and J. L. York, "Sprays formed by flashing liquid jets," *AIChE J.*, vol. 8, no. 2, pp. 149–153, May 1962, doi: 10.1002/aic.690080204.

[12] S. Li, Y. Zhang, and W. Qi, "Quantitative study on the influence of bubble explosion on evaporation characteristics of flash boiling spray using UV-LAS technique," *Exp. Therm. Fluid Sci.*, vol. 98, no. March, pp. 472–479, 2018, doi: 10.1016/j.expthermflusci.2018.03.025.

[13] E. M. Peter, A. Takimoto, and Y. Hayashi, "Flashing and Shattering Phenomena of Superheated Liquid Jets," *JSME Int. J. Ser. B*, vol. 37, no. 2, pp. 313–321, 1994, doi: 10.1299/jsmeb.37.313.

[14] H. Kamoun, G. Lamanna, B. Weigand, and J. Steelant, "High-speed shadowgraphy investigations of superheated liquid jet atomisation," in *ILASS-Americas 22nd Annual Conference on Liquid Atomization and Spray Systems*, 2010, no. May.

[15] G. Lamanna, H. Kamoun, B. Weigand, and J. Steelant, "Towards a unified treatment of fully flashing sprays," *Int. J. Multiph. Flow*, vol. 58, pp. 168–184, Jan. 2014, doi: 10.1016/j.ijmultiphaseflow.2013.08.010.

[16] Y.-I. Jin, H. J. Lee, K.-Y. Hwang, D.-C. Park, and S. Min, "Flashing injection of high temperature hydrocarbon liquid jets," *Exp. Therm. Fluid Sci.*, vol. 90, pp. 200–211, 2018, doi: https://doi.org/10.1016/j.expthermflusci.2017.09.016.

[17] Ł. J. Kapusta, R. Rogoz, J. Bachanek, Ł. Boruc, and A. Teodorczyk, "Low-Pressure Injection of Water and Urea-Water Solution in Flash-Boiling Conditions," *SAE Int. J. Adv. Curr. Pract. Mobil.*, vol. 3, no. 1, pp. 365–377, Sep. 2020, doi: https://doi.org/10.4271/2020-01-2110.

[18] Ł. J. Kapusta, "Understanding the collapse of flash-boiling sprays formed by multi-hole injectors operating at low injection pressures," *Energy*, vol. 247, p. 123388, 2022, doi: https://doi.org/10.1016/j.energy.2022.123388.

[19] N. Otsu, "A Threshold Selection Method from Gray-Level Histograms," *IEEE Trans. Syst. Man. Cybern.*, vol. 9, no. 1, pp. 62–66, Jan. 1979, doi: 10.1109/TSMC.1979.4310076.

[20] G. Zheng, W. Nie, S. Feng, and G. Wu, "Numerical Simulation of the Atomization Process of a Like-doublet Impinging Rocket Injector," *Procedia Eng.*, vol. 99, pp. 930–938, 2015, doi: https://doi.org/10.1016/j.proeng.2014.12.624.

[21] S. Li, Y. Zhang, W. Qi, and B. Xu, "Quantitative observation on characteristics and breakup of single superheated droplet," *Exp. Therm. Fluid Sci.*, vol. 80, pp. 305–312, 2017, doi: https://doi.org/10.1016/j.expthermflusci.2016.09.004.

[22] G. Brizi, L. Postrioti, and N. Van, "Experimental Analysis of SCR Spray Evolution and Sizing in High-Temperature and Flash Boiling Conditions." May 2019.